JOTCS A
Journal of the Turkish Chemical Society
Section: A
Chemistry
TURKISH CHEMICAL SOCIETY

Investigation of Electronic and Molecular Features of Zn_3S_3/PEG4000 Composite Using the DFT Method

Manahil A. Hraja[1], Aula M. Al Hindawi[1], Nagham M. Shiltagh[2*]

[1]Department of Chemistry, College of Education for Pure Science, University of Kerbala, Karbala, Iraq.
[2]Department of Physics, College of Science, University of Kerbala, Karbala, Iraq.

Abstract: Molecular geometry structures were accurately optimized to low convergence energy thresholds for the Zn_3S_3 cluster before and after adding Polyethylene Glycol (PEG4000). Density functional theory DFT/ B3LYP calculations with 6-113G (d, p) basis set were employed to investigate structural and electronic properties of Zn_3S_3/PEG4000 composite. The FTIR spectral lines were analyzed where an agreement of FTIR spectra of titled molecules was evaluated between experimental and theoretical findings of the active peaks of O–H, C–H, C=O, C–O–C, and Zn–S functional groups. The vibrational modes frequencies were systematically analyzed on the distribution basis of potential energy around the range 0–4000 cm^{-1} and observed 12 modes of vibrations for the Zn_3S_3 molecule, while 36 modes for the Zn_3S_3/PEG4000 compound. Frontier high occupied, and low unoccupied molecular orbitals (HOMO&LUMO) were calculated and plotted to obtain the energy gap (Eg) resulting from the difference between those orbitals. The promising indicator was obtained at increasing Eg from (4.031 to 4.459) eV after adding PEG4000, pointing out the effect of polymer on the ZnS surface as a capping agent. Additionally, electronic features of the mentioned structures, such as IP, EA, Ef, Eg, Cp, χ, η, S, and ω, were calculated. Finally, the molecular electrostatic potential (MEP) diagram of Zn_3S_3 and Zn_3S_3/ PEG4000 and charge densities of isosurface and contour diagrams were estimated, showing the nucleophilic and electrophilic attack of these compounds.

Keywords: PEG4000 polymer, ZnSNPs, HOMO&LUMO, Vibrational frequencies, DFT.

Submitted: September 7, 2023. **Accepted:** January 24, 2024.

Cite this: Hraja MA, Al Hindawi AM, Shiltagh NM. Investigation of Electronic and Molecular Features of Zn_3S_3/PEG4000 Composite Using the DTF Method. JOTCSA. 2024;11(2):565-74.

DOI: https://doi.org/10.18596/jotcsa.1356389

***Corresponding author's E-mail:** nagam.altememi@uokerbala.edu.iq

1. INTRODUCTION

Zinc sulfide (ZnS) is a substantial compound with a wide range of applications due to its unique optical and structural features. ZnS nanomaterials have a relatively large bandgap of 3.6 eV, which increases with decreasing particle size (1). In addition, 3D-Zn-VI used in semiconductors has drawn wide attention due to their applications in short-wavelength light-emitting devices. 3D-ZnS is one such binary compound that appears in two structures: the Wurtzite (WZ) structure at high temperatures and a cubic zinc alloy (ZB) structure at low temperatures and ambient pressures (2-4). Zinc is widely used on electrodes in the deposition process industry with other metals like Sn-alloy (5). The preparation of nanomaterials occupies a significant position in research centers, and the preparation methods have been varied, either physically or chemically, according to their application (6-8). Recently, polymers have played a vital role in improving and enhancing the characterizations of nanoparticles' surfaces (9,10). Polyethylene Glycol (PEG4000) is one of these polymers that is an ethereal compound belonging to the family of polymers with high molecular weight (11); some other names for the PEG4000

polymer include polyglycol, poly (ethylene oxide) (PEO), and poly (oxyethylene) (POE) (12). PEG is the most popular among the three types and the best among them to employ in the field of medicine and refers to polymers with molecular masses less than 20,000 g/mol. For instance, PEG 4000 is a safe and more effective drug compared to lactulose for the treatment of constipation in children (13), where several clinical studies have demonstrated that PEG 4000 is effective in the treatment of constipation in adults and children (14,15). In addition, PEG 4000 acts as an osmotic agent that increases fecal water content. PEG4000 is nontoxic and non-immunogenic (16). Thanks to the feature of PEG4000, it is flexible and soluble in water, so that it can work at high osmotic pressures (17,18). It has been proven that nanopolymers have the advantages of mass production and high stability, so the manufacture of smart or stimuli-responsive polymers has been achieved. Either from natural or synthetic resources, one of the most important natural polymers used in the manufacture of medical preparations is dextrose gelatin. In contrast, synthetic polymers use polyethylene glycol (19,20). Density Functional Theory (DFT), which is an algorithm of quantum mechanical modeling utilized in the chemical and physical fields to discover electronic structure (21), has established itself as a valuable research tool to validate experimental conclusions or characterize those possibilities left open (22).

Computational processes offer precisely superior scales in chemical interactions and combinations phenomena, particularly (DFT) method, which theoretically presents predictions of material design through the geometrical structures (23) in addition to the low cost. Furthermore, the more quantitative predictions of phenomena that are made and confirmed by experiment, the more the overall theory is accepted when the theoretical investigation is "confirmed" for that specific experiment (24). Nevertheless, several theoretical studies have been relied on and taken into account in practical applications such as gas sensors (25).

DFT theory was recently employed to study the structural and electronic properties of ZnS molecules as a nanotube in different numbers of ZnS atoms (26,27), or by ab initio/DFT to study electronic and spectroscopic properties of ZnO-NPs. Furthermore, an investigation of Polyethylene Glycol (PEG) was based on a nanocomposite by DFT study to use as a drug in medical applications (23). On the other hand, to study the effect of polymers on nanoparticle behaviors, the structural and electronic properties of ZnS nanoparticles with the presence of PEG4000 have been investigated experimentally in our recent work (28). However, their structural, electronic, and vibrational features have not been theoretically investigated. Therefore, this work could be promising for gaining more knowledge for this composite over theoretical study using the DFT theory.

2. COMPUTATIONAL DETAILS

The development of the quantum mechanical technique has been influenced by the density functional theory (DFT), which has been used to study the electronic structure and behavior of many electron systems. Disciplines of physics and chemistry employ functional analysis to gain an understanding of the electron density distribution. A many-electron system's ground state (GS) and other features can be identified using DFT, as demonstrated by this study. The most popular and adaptable method in computational physics and chemistry disciplines is, by far, DFT. Additionally, it has proven to be quite efficient at estimating the properties of materials in their ground state. The approach in this work uses DFT theory with hybrid B3LYP (Becke, three parameters, Lee-Yang-Parr) and a basis set with 6-311G**. Where the first asterisk above basis G represents the polarization set d-function for heavy atoms. However, the second sign indicates the polarization of p-functions of hydrogen atoms or sometimes must be written as 6-311G (d, p) (29,30). Because of the accuracy of this basis set, it was powerfully used to calculate energetic and electronic features in multiple phases (31). All those equations and theories were involved by Gaussian 09 and Gaussian View 6.0 software (32).

To achieve accurate results, the geometries of molecules were optimized precisely to lower the convergence thresholds. Furthermore, Frequencies of normal vibrations were calculated to confirm the minimal energy at geometric optimization by solving the self-consistent field (SCF) equation.

Figure (1-a) demonstrates the molecular structure of a cluster of three Zn atoms and three S atoms (Zn_3S_3); either (1-b) clarifies the cluster of Zn_3S_3 after adding PEG4000 polymer $(C_2H_4O)_n$, as adsorption process experimentally on PEG surface. These structures were optimized geometrically at the following conditions: maximum force, RMS force, max. displacement and RMS displacement converged at several steps, 0.000076, 0.000021, 0.000104, and 0.000099, respectively. Figure (2) shows the steps of geometrical optimization.

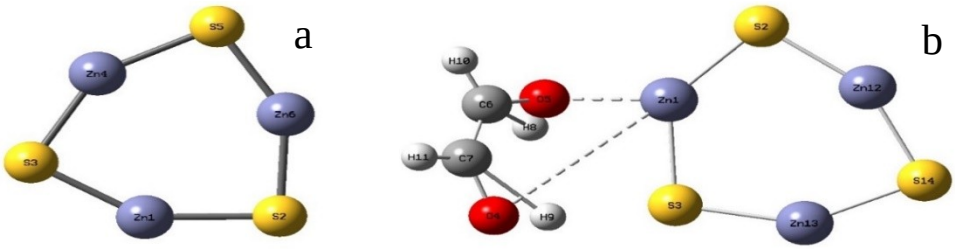

Figure 1: The optimized structures of ZnSNPs (Zn_3S_3) before adding PEG4000 (a), and after adding the polymer (b) using the DFT method with basis set 6-311G**.

The electronic features of the mentioned molecules were computed, which are Fermi level energy (Ef), Energy of bandgap (Eg), and Ionization potential (IP) that represents the amount of energy needed to break the structural unit of the weakest electron bond to the nucleus. The greater the ionization energy, the more difficult it is to extract the electron and electron affinity (*EA*), which is the amount of energy released when an electron is added to a gaseous atom, after identifying the Highest Occupied Molecular Orbital (HOMO) and Lowest Unoccupied Molecular Orbital (LUMO) energies by the following equations (33,34):

$$Eg = E_{LUMO} - E_{HOMO} \quad (1)$$

$$IP = - E_{HOMO} \quad (2)$$

$$EA = - E_{LUMO} \quad (3)$$

$$Ef = (E_{HOM} + E_{LUMO}) / 2 \quad (4)$$

In addition, to describe the chemical reactivity of the studied system between polymer-NPs, the quantum molecular identifiers (Cp, χ , η, S, and ω) were employed. These descriptors involved are generally: the chemical potential (Cp) is the energy that can be absorbed or released due to a change in the number of particles, and it can be known as the ferry energy in a semiconductor when a system of electrons at a temperature of absolute zero, electronegativity (χ) is a measure of an atom's ability to attract electrons in a chemical bond; the global hardness (η), the softness (S), and the electrophilicity index (ω) are by the following equations (35, 36):

$$Cp = - \chi \quad (5)$$

$$\chi = IP+EA / 2 \quad (6)$$

$$\eta = IP-EA /2 \quad (7)$$

$$S = 1/ \eta \quad (9)$$

$$\omega = - \chi^2 / 2\eta \quad (10)$$

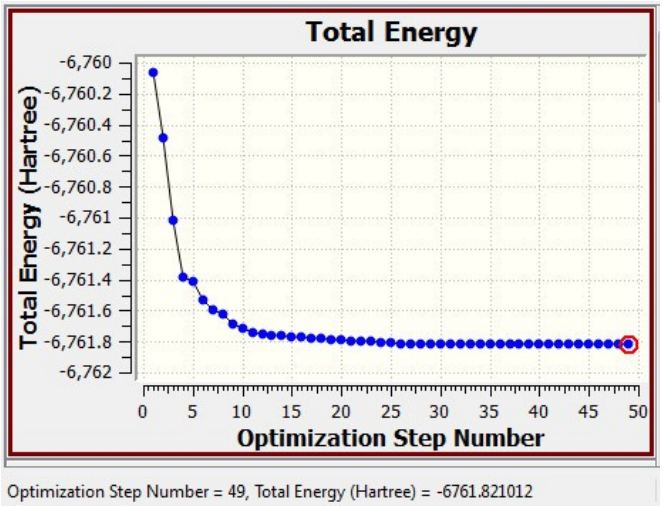

Figure 2: Steps of geometrical optimization with minimal energy DFT study using B3LYP-D/6–311 G.

3. RESULTS AND DISCUSSION

3.1. Vibrational Frequencies & FTIR spectra

Any way of connection with Ethelyne Glygole polymer is a planar structure of the C1 point symmetry group. According to the equation (3N-6) for non-linear molecules, the number of normal vibration modes can be calculated, where N is the number of atoms. Hence, twelve vibrational modes were obtained for the Zn_3S_3 molecule, which consists of 6 atoms. These frequencies have been arranged in Table (1) from the lowest frequency of the patterns to the highest mode. The highest frequency modes are (11 and 12) in the range (408.23-408.89) cm^{-1}. In comparison, 36 modes were obtained for the Zn_3S_3/PEG4000 structure, including 14 atoms. The strongest modes at high frequencies are (33, 34, 35, and 36) at frequencies (3175.62, 3244.59, 3450.37, 374.07) $cm^{-1,}$ respectively, as shown in Table (2).

On the other hand, the IR spectra of the studied structure were calculated at the range (0 – 4000) cm^{-1} using DFT-B3LYP levels with the 6-311G** basis set. The comparison of the FT-IR spectra between theoretical and experimental spectra is illustrated in Figure (3) for Zn_3S_3 and Zn_3S_3/PEG, observing a strong agreement between them.

Table 1: The range of normal vibrational modes for Zn_3S_3 from lowest to highest frequency.

No. Mode	Frequency/ cm^{-1}	No. Mode	Frequency/ cm^{-1}
MODE 1	89.33	MODE7	297.88
MODE2	90.87	MODE8	298.05
MODE3	106.96	MODE9	327.78
MODE4	107.06	MODE10	387.43
MODE5	146.05	MODE11	408.23
MODE6	170.53	MODE12	408.89

Table 2: The range of normal vibrational modes for Zn_3S_3/PEG400 from lowest to highest frequency.

No. Mode	Frequency/cm^{-1}	No. Mode	Frequency/cm^{-1}	No. Mode	Frequency/cm^{-1}
MODE 1	16.59	MODE 13	278.38	MODE 25	945.70
MODE 2	37.60	MODE 14	297.00	MODE 26	964.47
MODE 3	67.18	MODE 15	309.08	MODE 27	1138.66
MODE 4	80.75	MODE 16	335.13	MODE 28	1271.64
MODE 5	87.68	MODE 17	372.38	MODE 29	1322.46
MODE 6	98.75	MODE 18	393.31	MODE 30	1393.98
MODE 7	105.80	MODE 19	416.68	MODE 31	1407.61
MODE 8	120.49	MODE 20	431.47	MODE 32	1713.20
MODE 9	130.08	MODE 21	530.63	MODE 33	3175.62
MODE 10	154.22	MODE 22	666.68	MODE 34	3244.59
MODE 11	167.68	MODE 23	721.17	MODE 35	3450.37
MODE 12	257.22	MODE 24	767.55	MODE 36	3764.07

It was found that the broad peaks at frequency 3760 cm^{-1} (DFT) and frequency 3480 cm^{-1} belong to the black line (ZnS/PEG4000 (exp.)), indicating to the OH-stretching vibrations band (37, 38). This stretching vibration is significantly attributed to the hydrogen bonding (39). Meanwhile, this band for ZnS (exp.) in the pink line has red-shifted to the short frequency 3221 cm^{-1} (long wavelength) due to the confinement quantum of phonon (26). This could be evidence of the effect of polymer that enhances the nano properties of ZnS particles.

In addition, the peaks of (1120 and 1110) cm^{-1} for Zn_3S_3/PEG4000 (DFT) and ZnS/PEG4000 (Exp), respectively, indicate the C–O–C band stretching vibrations (40). Other signed Peaks at (660, 657, and 648) cm^{-1} are attributed to the stretching vibrations of the Zn–S bond and belong to the Zn_3S_3/PEG4000 (DFT), ZnS/PEG4000 (Exp), and Zn_3S_3 (DFT) respectively (41, 42). It was observed that the peaks of vibration bands at regions (416, 416, and 420) cm^{-1} belong to (ZnS/PEG4000 (exp.), Zn_3S_3/PEG 4000 (DFT), and ZnS (exp.), respectively. Also, it is located at the range around 600 cm^{-1}, where the range of the appearance of the Zn–S bond is located around the range 450–1000. Agrees with Liu et. Al.'s work (43). Table (3) presents this comparison of FTIR spectra of mentioned molecules.

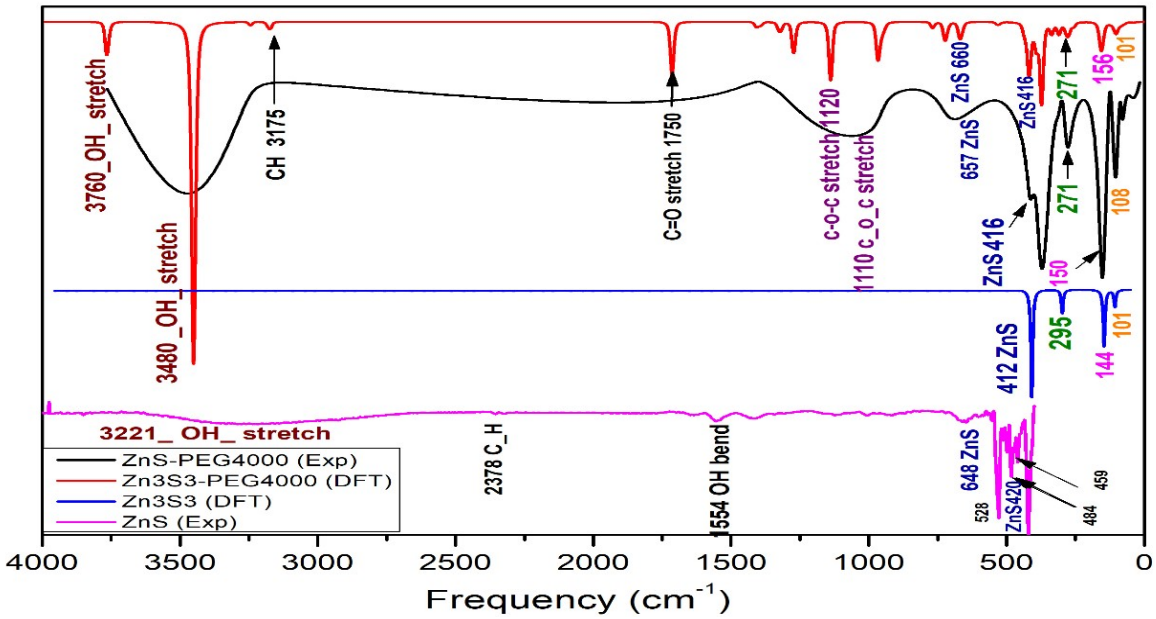

Figure 3: Comparison of the FTIR spectra for ZnSNPs before and after adding PEG polymer theoretically and experimentally showing remarkable agreement between them.

Table 3: Comparison of FTIR of studied structures between experimental and theoretical spectra for ZnSNPs before and after adding PEG polymer clarifying the range of functional groups.

ZnS/PEG (Exp)		**Zn_3S_3/PEG (DFT)**		**ZnS (Exp)**		**Zn_3S_3 (DFT)**	
Functional group	The range	Functional group	The range	Functional group	The range	Functional group	The range
Zn – S	657–416	Zn–S	660–416	Zn – S	648–416	Zn – S	412
C– O –C	1110	C– O –C	1120				
O – H	3760	O – H	3480	O – H	3221		

3.2. Electronic Properties

Molecular orbital theory (MOT) is a significantly sophisticated model that covers comprehensive aspects relating to the bonding of orbitals, energies, chemical reactions, and their characterizations. From these orbitals are the highest occupied molecular orbital (HOMOs) which occupies by electrons in it and have the highest energy. The other one is the lowest unoccupied molecular orbital (LUMO), which has no electrons and the lowest energy. The values of those molecular orbitals were computed for ZnSNPs before and after adding PEG polymer using the DFT method with a 6-113G** basis set. By determining the HOMO, LUMO energies and the HOMO-LUMO (*Eg*) that are a valuable index of the interaction system, electronic properties *IP, EA, Ef, Eg, Cp, χ, η, S* and *ω*, were calculated using the (1–10) Equations. Table (4) demonstrates the electronic properties of ZnS–NP clusters before and after adding PEG4000 at room temperature. It was observed an agreement of *Eg* experimentally and theoretically around 4.2 (grey shaded) and 4.03 eV, respectively, for the ZnS cluster. Similarly, there are (4.5 eV - exp) and (4.459 eV - DFT) concerning ZnS-PEG. Figure (4) clarifies HOMO and LUMO MOs for mentioned molecules, where the energy gap (*Eg*) increases with adding polymer, indicating the effect of the PEG molecule on the ZnS particles as a capping agent, indicating the quantum confinement concept strongly, the greater value for the band gap (the smallest nanoparticle diameter) (44).

Table 4: Computed electronic features of ZnSNPs before and after adding PEG polymer at room temperature.

Properties	Zn_3S_3 (DFT)	Zn_3S_3 /PEG (DFT)
E_{HOMO}	- 7.0199	- 6.7014
E_{LUMO}	- 2.9886	- 2.2323
Ef / eV	- 5.0043	- 4.4668
Eg/ eV	4.0310	4.4599
Eg / eV	4.2000 (Exp)	4.5000 (Exp)
IP / eV	7.0199	6.7014
EA / eV	2.9886	2.2323
Cp / eV	- 5.0043	- 4.4668
χ / eV	5.0043	4.4668
η / eV	2.0156	2.2323
S / $(eV)^{-1}$	0.4961	0.4479
ω / eV	- 6.2122	- 4.4691

3.3. Molecular Electrostatic Potential

To evaluate the connections and interactions of non-covalent inside molecules with intermolecular distance and to examine the attractive or repulsive interactions, nonlocalized dispersion among the structures reactions, molecular electrostatic potential (MEP) diagram, and densities of the electron with charge were utilized (45) using B3LYP calculations with basis set 6-311G(d,p). The zones of these interactions were described in Figure (5) for a titled molecule to visualize three interaction areas based on the electron density function (46).

The being of hydrogen bonding is presented in blue zones. Red patches indicate the repulsive interactions and the green zones refer to the Van der Waals bonding (VdW) (46). Figure (5) shows the transfor-mation of the colored from a cluster of Zn_3S_3 into Zn_3S_3/PEG4000 (a to b), respectively. Furthermore, The advantage of the molecular electrostatic potential scheme is that it is a useful tool for investigating reactivity to electrophilic or nucleophilic attacks in the studied systems depending on the charge distribution. The colored line shown in the upper edge in Fig. (5) is color-coded of the system referring to two regions (the range from -8.065×10^{-2} (red) to 8.065×10^{-2} (blue) and from -4.036×10^{-4} to 4.036×10^{-4} for ZnS cluster and Zn_3S_3-PEG-4000 surfaces respectively; the negative charge densities in red color represent the acceptor of the H-bonding of molecules. Meanwhile, the second zone demonstrates positive charge densities in the blue ruler for the donor of the H-bonding (47).

On the other hand, If all Zn_3S_3/PEG4000 surfaces are plotted with all iso-surface values, only the top surface will be seen. To see all the studied molecules' surfaces, it can simply plot each surface as a contour around the molecule, as shown in Figures (5- c and d) for the Zn_3S_3 cluster and Zn_3S_3/PEG4000 surface, respec-tively.

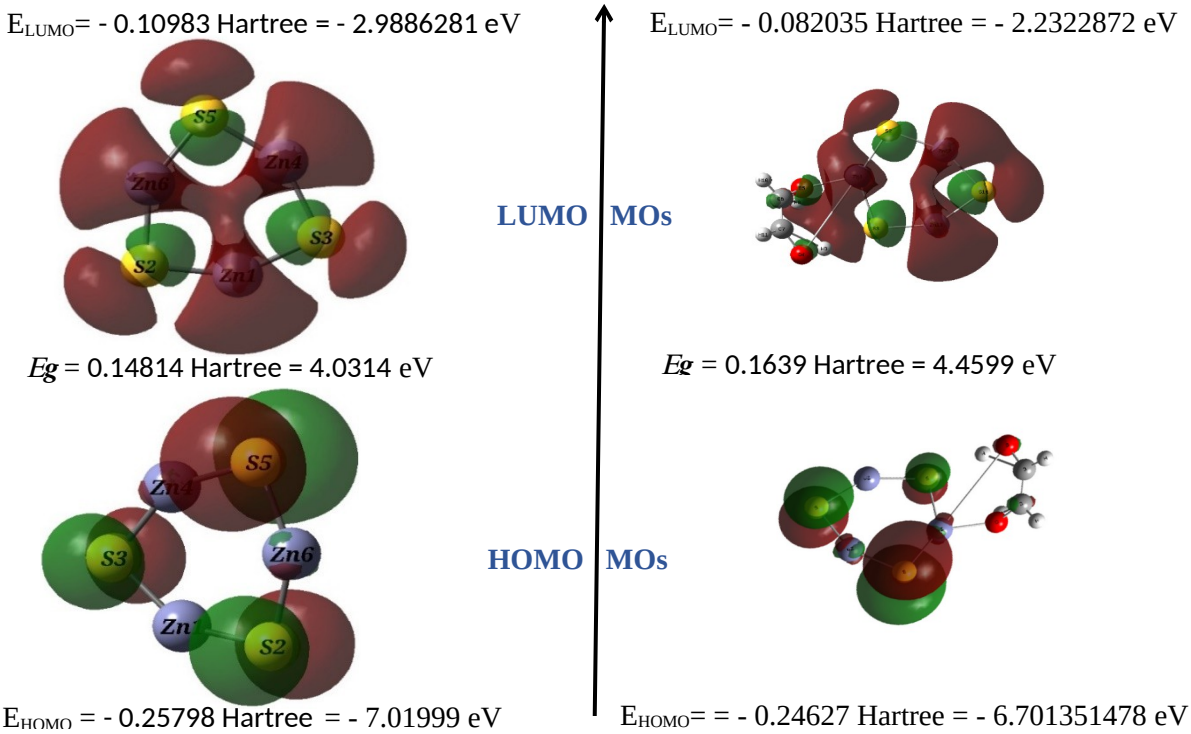

Figure 4: Frontier molecular (HOMO&LUMO) orbitals and E*g* of ZnSNPs cluster (on left), for Zn_3S_3/PEG4000 (on right). An increase in E*g* around 0.43 eV with adding PEG polymer indicates the enhancement for nano features.

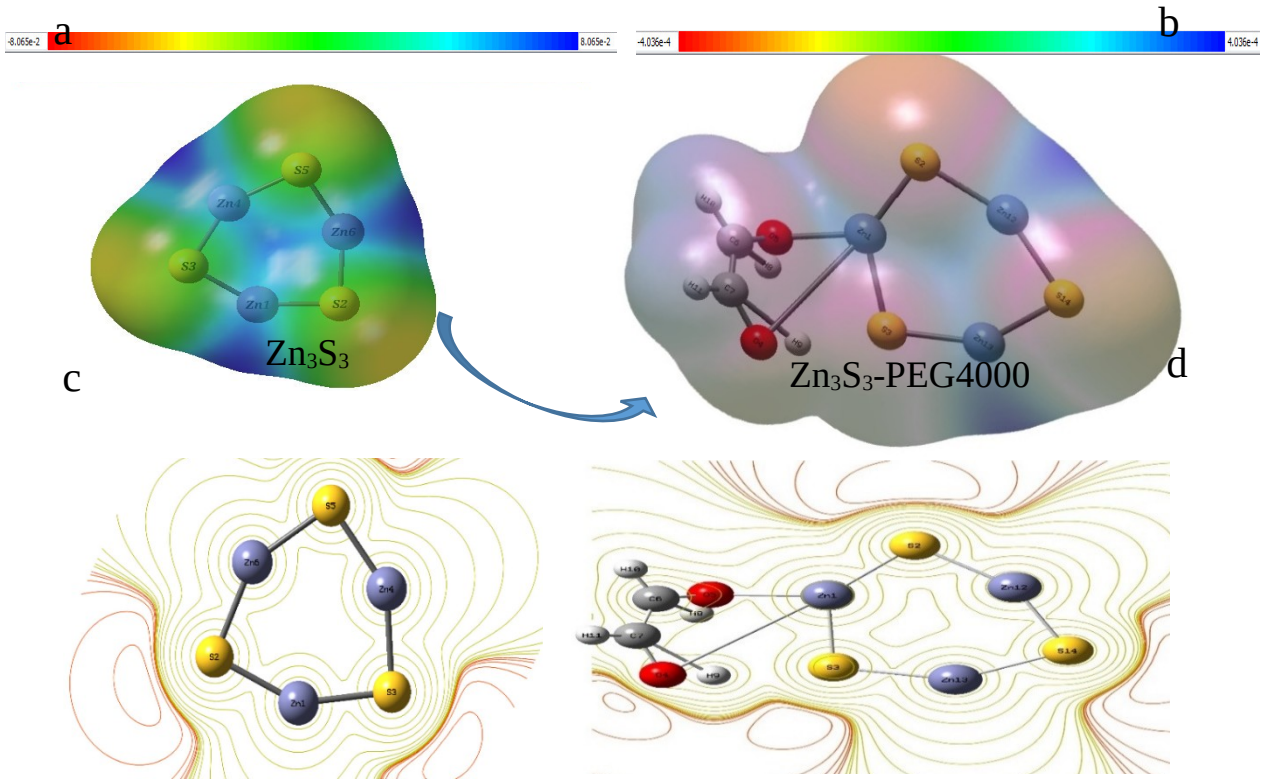

Figure 5: Charge density distribution as color-coded ruler in upper edge (red color for negative charge and blue for positive), MEP isosurface surfaces diagram of Zn_3S_3 (a) Zn_3S_3_PEG4000 (b), MEP contour surface of Zn_3S_3 (c) Zn_3S_3_PEG4000 (d).

4. CONCLUSION

Structural and electronic features of a cluster of three atoms of Zn and three atoms of S (Zn_3S_3) have been calculated theoretically for the first time using the DFT computations with the hybrid B3LYP and 6-311G (d, p) basis set. The same calculations have been conducted for the mentioned molecule after adding the PEG4000 polymer (Zn_3S_3/PEG4000). The spectral lines, such as FTIR spectra, were analyzed, and a comparison has been made between the two structures experimentally and theoretically. A strong agreement of active peak position between experimental and theoretical spectra was found.

Vibrational frequencies assigned around the range 0–4000 cm^{-1} were systematically analyzed, and 12 modes of vibration of the Zn_3S_3 molecule and 36 modes of the Zn_3S_3/PEG4000 compound were observed. In addition, the energies of HOMO and LUMO orbitals were calculated and illustrated to evaluate the Energy gap (*Eg*). A remarkable effect of the polymer after adding to the ZnS cluster was noticed on the Energy gap, where the gap increases from (4.031 to 4.459) eV, and these findings are in agreement with the experimental value indicating the quantum confinement concept strongly, the greater value for the band gap (the smallest nan particle diameter). The molecular electrostatic potential (MEP) diagram and charge densities of isosurface and contour diagrams were estimated, showing these compounds' nucleophilic and electrophilic attack.

5. ACKNOWLEDGMENTS

The authors would like to thank the Department of Chemistry, College of Education for Pure Science, University of Kerbala, and the Department of Physics, College of Science, University of Kerbala, for supporting this work.

6. CONFLICTS OF INTEREST

The authors declared no conflict of interest.

7. REFERENCES

1. Hamad S, Catlow CRA. Computational study of the relative stabilities of ZnS clusters, for sizes between 1 and 4nm. J Cryst Growth [Internet]. 2006 Aug 15;294(1):2–8. Available from: <URL>.

2. Lashgari H, Boochani A, Shekaari A, Solaymani S, Sartipi E, Mendi RT. Electronic and optical properties of 2D graphene-like ZnS: DFT calculations. Appl Surf Sci [Internet]. 2016 Apr 30;369:76–81. Available from: <URL>.

3. Abd-Alameer Jawad S, Ali Ahmed H. Synthesis, Characterization and Study of Amide Ligand Type N_2S_2 and Metal Complexes with Di Valance Manganese, Zinc and tri Valance Iron. Ann Rom Soc Cell Biol [Internet]. 2021 Apr 2;25:8511–20. Available from: <URL>.

4. Wang Z, Daemen LL, Zhao Y, Zha CS, Downs RT, Wang X, et al. Morphology-tuned wurtzite-type ZnS nanobelts. Nat Mater [Internet]. 2005 Dec 1;4(12):922–7. Available from: <URL>.

5. Alesary HF, Ismail HK, Shiltagh NM, Alattar RA, Ahmed LM, Watkins MJ, et al. Effects of additives on the electrodeposition of Zn Sn alloys from choline chloride/ethylene glycol-based deep eutectic solvent. J Electroanal Chem [Internet]. 2020 Oct 1;874:114517. Available from: <URL>.

6. Turki ZT, Al Hindawi AM, Shiltagh NM. Green Synthesis of CdS Nanoparticles using Avocado Peel Extract. NanoWorld J [Internet]. 2022;08(03). Available from: <URL>.

7. Shiltagh NM, Ridha NJ, Hindawi AM Al, Tahir KJ, Madlol RA, Alesary HF, et al. Studying the optical properties of silver nitrates using a pulsed laser deposition technique. In: AIP Conference Proceedings [Internet]. American Institute of Physics Inc.; 2020. p. 050059. Available from: <URL>.

8. Al Hindawi AM, Obaid NH, Juadah I, Shiltagh N, Tahit KJ. Fabrication and Characterization of Silver Nanoparticles Using Plant Extract. Int J Pharm Res [Internet]. 2020 Mar 1;12(2):985–8. Available from: <URL>.

9. Jawad RA, Shiltagh N, Aboud LH, Watkins MJ. The Effect of Silver Nanoparticles on a Mixture of MB-dye/PVA-Polymer as Determined by Absorption and Emission Spectra Measurements. NanoWorld J [Internet]. 2021;7(1):13–21. Available from: <URL>.

10. Tahir KJ, Obeed HH, Shiltagh NM. Study optical properties of R6G dye doped in polymer PVA. J Phys Conf Ser [Internet]. 2019 Jul 1;1234(1):012048. Available from: <URL>.

11. Brittain WJ, Minko S. A structural definition of polymer brushes. J Polym Sci Part A Polym Chem [Internet]. 2007 Aug 15;45(16):3505–12. Available from: <URL>.

12. Almashhadani NJH. UV-Exposure effect on the mechanical properties of PEO/PVA blends. Iraqi J Sci [Internet]. 2021 Jul 2;62(6):1879–92. Available from: <URL>.

13. Wang Y, Wang B, Jiang X, Jiang M, Xu C, Shao C, et al. Polyethylene glycol 4000 treatment for children with constipation: A randomized comparative multicenter study. Exp Ther Med [Internet]. 2012 May 17;3(5):853–6. Available from: <URL>.

14. Corazziari E, Badiali D, Habib FI, Reboa G, Pitto G, Mazzacca G, et al. Small volume isosmotic polyethylene glycol electrolyte balanced solution (PMF-100) in treatment of chronic nonorganic constipation. Dig Dis Sci [Internet]. 1996 Aug;41(8):1636–42. Available from: <URL>.

15. Pashankar DS, Bishop WP. Efficacy and optimal dose of daily polyethylene glycol 3350 for treatment of constipation and encopresis in children. J Pediatr [Internet]. 2001 Sep 1;139(3):428–32. Available from: <URL>.

16. Keerthana M, Komala G, Nagaraju R. Polymeric Micelles of Oregano - Formulation and In-Vitro Evaluation. Curr Trends Biotechnol Pharm [Internet]. 2023 Feb 20;17(1):660–70. Available from: <URL>.

17. Chen X, Liu G, Zhao L, Du L, Xie J, Wei D. *Lactiplantibacillus plantarum* X7022 ameliorates loperamide-induced constipation and modulates gut microbiota in mice. Food Bioeng [Internet]. 2022 Dec 2;1(3–4):252–63. Available from: <URL>.

18. Wu LC, Zheng ED, Sun HY, Lin XZ, Pan JY, Lin XX. Observation of the application effect of low-volume polyethylene glycol electrolyte lavage solution (PEG-ELS) combined with ascorbic acid tablets in bowel preparation for colonoscopy in hospitalized patients. Front Oncol [Internet]. 2023 Apr 14;13:1038461. Available from: <URL>.

19. Yu Z, Shen X, Yu H, Tu H, Chittasupho C, Zhao Y. Smart Polymeric Nanoparticles in Cancer Immunotherapy. Pharmaceutics [Internet]. 2023 Feb 26;15(3):775. Available from: <URL>.

20. Figueiredo AQ, Rodrigues CF, Fernandes N, de Melo-Diogo D, Correia IJ, Moreira AF. Metal-Polymer Nanoconjugates Application in Cancer Imaging and Therapy. Nanomaterials [Internet]. 2022 Sep 13;12(18):3166. Available from: <URL>.

21. Rahimi R, Solimannejad M. Empowering hydrogen storage performance of B_4C_3 monolayer through decoration with lithium: A DFT study. Surfaces and Interfaces [Internet]. 2022 Apr 1;29:101723. Available from: <URL>.

22. Huang EW, Lee WJ, Singh SS, Kumar P, Lee CY, Lam TN, et al. Machine-learning and high-throughput studies for high-entropy materials. Mater Sci Eng R Reports [Internet]. 2022 Jan 1;147:100645. Available from: <URL>.

23. Adekoya OC, Adekoya GJ, Sadiku RE, Hamam Y, Ray SS. Density Functional Theory Interaction Study of a Polyethylene Glycol-Based Nanocomposite with Cephalexin Drug for the Elimination of Wound Infection. ACS Omega [Internet]. 2022 Sep 27;7(38):33808–20. Available from: <URL>.

24. Huang B, von Lilienfeld OA, Krogel JT, Benali A. Toward DMC Accuracy Across Chemical Space with Scalable Δ-QML. J Chem Theory Comput [Internet]. 2023 Mar 28;19(6):1711–21. Available from: <URL>.

25. Alaa Hussein T, Shiltagh NM, Kream Alaarage W, Abbas RR, Jawad RA, Abo Nasria AH. Electronic and optical properties of the BN bilayer as gas sensor for CO_2, SO_2, and NO_2 molecules: A DFT study. Results Chem [Internet]. 2023 Jan 1;5:100978. Available from: <URL>.

26. Hussein MT, Thjeel HA. Vibration Properties of ZnS

nanostructure Wurtzoids: ADFT Study. J Phys Conf Ser [Internet]. 2019 Feb 1;1178(1):012015. Available from: <URL>.

27. Hussain MT, Thjeel HA. Study of geometrical and electronic properties of ZnS wurtzoids via DFT. Chalcogenide Lett [Internet]. 2018;15(10):523–8. Available from: <URL>.

28. Hraja MA, Al Hindawi AM, Shiltagh NM. Synthesis, Characterization And Studying The Optical Properties Of Zinc Sulfide Nanoparticles In The Presence Of Peg4000. J Aeronaut Mater. 2023;43:37–48.

29. Becke AD. Density-functional thermochemistry. III. The role of exact exchange. J Chem Phys. 1993 Apr 1;98(7):5648–52. Available from: <URL>.

30. Lee C, Yang W, Parr RG. Development of the Colle-Salvetti correlation-energy formula into a functional of the electron density. Phys Rev B Condens Matter [Internet]. 1998;37:785–9. Available from: <URL>.

31. Sadoon AM. Theoretical Investigation of the Structures and Energetics of (MX)-Ethanol Complexes in the Gas Phase. J Turkish Chem Soc Sect A Chem [Internet]. 2023 Feb 28;10(1):47–54. Available from: <URL>.

32. Pople JA, Gill PMW, Johnson BG. Kohn—Sham density-functional theory within a finite basis set. Chem Phys Lett [Internet]. 1992 Nov 20;199(6):557–60. Available from: <URL>.

33. Parey V, Jyothirmai MV, Kumar EM, Saha B, Gaur NK, Thapa R. Homonuclear B_2/B_3 doped carbon allotropes as a universal gas sensor: Possibility of CO oxidation and CO_2 hydrogenation. Carbon N Y [Internet]. 2019 Mar 1;143:38–50. Available from: <URL>.

34. Huang Y, Rong C, Zhang R, Liu S. Evaluating frontier orbital energy and HOMO/LUMO gap with descriptors from density functional reactivity theory. J Mol Model [Internet]. 2017 Jan 8;23(1):3. Available from: <URL>.

35. Kaufman GB. Inorganic chemistry: principles of structure and reactivity, 4th ed. (Huheey, James E.; Keiter, Ellen A.; Keiter, Richard L.). J Chem Educ. 1993 Oct 1;70(10):A279. Available from: <URL>.

36. De Proft F, Geerlings P. Conceptual and Computational DFT in the Study of Aromaticity. Chem Rev [Internet]. 2001 May 1;101(5):1451–64. Available from: <URL>.

37. Kaur J, Sharma M, Pandey OP. Photoluminescence and photocatalytic studies of metal ions (Mn and Ni) doped ZnS nanoparticles. Opt Mater (Amst) [Internet]. 2015 Sep 1;47:7–17. Available from: <URL>.

38. Kharazmi A, Faraji N, Mat Hussin R, Saion E, Yunus WMM, Behzad K. Structural, optical, opto-thermal and thermal properties of ZnS–PVA nanofluids synthesized through a radiolytic approach. Beilstein J Nanotechnol [Internet]. 2015 Feb 23;6:529–36. Available from: <URL>.

39. Abdelmoulahi H, Ghalla H, Nasr S, Bahri M, Bellissent-Funel MC. Hydrogen-bond network in liquid ethylene glycol as studied by neutron scattering and DFT calculations. J Mol Liq [Internet]. 2016 Aug 1;220:527–39. Available from: <URL>.

40. Pretsch E, Bühlmann P, Badertscher M. Structure Determination of Organic Compounds. Berlin, Heidelberg: Springer Berlin Heidelberg; 2020. Available from: <URL>.

41. Yang H, Holloway PH, Ratna BB. Photoluminescent and electroluminescent properties of Mn-doped ZnS nanocrystals. J Appl Phys [Internet]. 2003 Jan 1;93(1):586–92. Available from: <URL>.

42. Nanaki SG, Kyzas GZ, Tzereme A, Papageorgiou M, Kostoglou M, Bikiaris DN, et al. Synthesis and characterization of modified carrageenan microparticles for the removal of pharmaceuticals from aqueous solutions. Colloids Surfaces B Biointerfaces. 2015 Mar;127:256–65. Available FROM: <URL>.

43. Liu LN, Dai JG, Zhao TJ, Guo SY, Hou DS, Zhang P, et al. A novel Zn(II) dithiocarbamate/ZnS nanocomposite for highly efficient Cr^{6+} removal from aqueous solutions. RSC Adv [Internet]. 2017 Jul 12;7(56):35075–85. Available from: <URL>.

44. Bhargava RN, Gallagher D, Hong X, Nurmikko A. Optical properties of manganese-doped nanocrystals of ZnS. Phys Rev Lett [Internet]. 1994 Jan 17;72(3):416–9. Available from: <URL>.

45. Shamim M, Perveen M, Nazir S, Hussnain M, Mehmood R, Khan MI, et al. DFT study of therapeutic potential of graphitic carbon nitride (g-C_3N_4) as a new drug delivery system for carboplatin to treat cancer. J Mol Liq [Internet]. 2021 Jun 1;331:115607. Available from: <URL>.

46. Noureddine O, Issaoui N, Medimagh M, Al-Dossary O, Marouani H. Quantum chemical studies on molecular structure, AIM, ELF, RDG and antiviral activities of hybrid hydroxychloroquine in the treatment of COVID-19: Molecular docking and DFT calculations. J King Saud Univ - Sci [Internet]. 2021 Mar 1;33(2):101334. Available from: <URL>.

47. Adekoya OC, Adekoya GJ, Sadiku ER, Hamam Y, Ray SS. Application of DFT Calculations in Designing Polymer-Based Drug Delivery Systems: An Overview. Pharmaceutics [Internet]. 2022 Sep 19;14(9):1972. Available from: <URL>.